Materials Science Forum Vols. 299-300 (1999) pp 141-148

doi:10.4028/www.scientific.net/MSF.299-300.141

Use of Rare Earth Concentrate as a SiAlON Sintering Additive

I.R. Ruiz, A.H. Bressiani and J.C. Bressiani

Instituto de Pesquisas Energéticas e Nucleares - IPEN, Travessa R, 400, Cidade Universitária, CEP 05508-900, S. Paulo, SP, Brazil
E-Mail: iruiz@net.ipen.br

Keywords: Covalent Ceramics, SiAlON, Sintering and Microstructure

ABSTRACT. The sintering additive used in SiAlON containing 5, 10, 15 and 20 eq% Al was a concentrate of rare earth elements, with 89.5% Y_2O_3, 3.9% Er_2O_3, 3.8% Dy_2O_3, 1.8% Lu_2O_3 and other rare earth elements at lower concentrations. The sintering variables studied were: Al content in solid solution with SiAlON, heating rate, sintering time and temperature. The results show that an increase in Al concentration leads to higher densities and $\alpha \rightarrow \beta$ transformation, and smaller grains with more spherical shape. An increase in both sintering time and temperature and heating rate lead to the formation of larger grains with smaller aspect ratio. Samples sintered at 1700 °C/30 min had higher density values. Samples with 99% of theoretical density were obtained by using the concentrate of rare earth elements.

INTRODUCTION

It is very difficult to densify Si_3N_4 by diffusional solid state mechanisms, largely applied in oxide ceramics, due to the high directional feature of covalent bonding and high vapor pressure at high temperatures.

The most used method to improve Si_3N_4 densification is the addition of metallic oxides. This method leads to SiAlON systems obtained by controlled additions of Al_2O_3 and AlN in Si_3N_4. The sintering process occurs by liquid phase formation in which α-Si_3N_4 dissolves, and β-Si_3N_4 is precipitated with simultaneous substitution of Si^{+4} by Al^{+3} and N^{-3} by O^{-2}. The resulting compound is a solid solution which has the general formula $Si_{6-x}Al_xO_xN_{8-x}$ (x varying from 0 to 4.2). This material is used for cutting tools, special mechanical sealing, engine components and many other applications, due to the easiness to obtain density values closer to the theoretical ones.

The SiAlON sinterability can be improved if Y_2O_3, CeO_2 or other rare earth oxides are added. By controlling the additives it is possible to obtain dense bodies just by pressureless sintering. In this work, the influence of heavy rare earth concentrate addition with 89% Y_2O_3 on the SiAlON densification and microstructural development was studied.

ANALYTICAL PROCEDURES

In order to obtain samples with additives homogeneously distributed, Al_2O_3 and rare earth concentrates [$(REC)_2O_3$] were powdered in ball mill for 24 hours, with isopropyl alcohol. After drying, Si_3N_4 and AlN were added and mixed in Turbula mixer for 3 hours with isopropyl alcohol in quantities enough to obtain SiAlON with 5, 10, 15 and 20 eq% Al and 5 wt.% $(REC)_2O_3$, named β5-C5, β10-C5, β15-C5 and β20-C5, respectively. The compositions of studied samples are shown in Table 1.

The powder was uniaxially pressed (50 MPa) in a pellet shape with 7 mm diameter and 10 mm thickness, followed by cold-isostatic pressing (200 MPa).

In order to study the densification behavior, the dimensional change ($\Delta L/L_0$) was measured in a Netzsch dilatometer with graphite resistance under nitrogen atmosphere. The sintering parameters were: composition, heating rate (5 or 20 °C/min), dwell temperature (1700 or 1750 °C) and sintering time (30 or 60 minutes). The parameters are shown in Table 2.

X-Ray diffraction (CuKα), Scanning Electron Microscopy, Energy Dispersive Spectroscopy (EDX) and hydrostatic methods were used to determine crystalline phases, microstructure features, main atomic elements and densities, respectively.

Table 1 - Compositions of samples.

Sample	Si_3N_4 (wt%)	AlN (wt%)	Al_2O_3 (wt%)	$(CTR)_2O_3$ (wt%)
β5-C5	89.150	3.583	2.267	5.000
β10-C5	83.073	5.312	6.615	5.000
β15-C5	77.193	6.984	10.823	5.000
β20-C5	71.502	8.602	14.896	5.000

Table 2 - Sintering parameters.

Sample	Temperature (°C)	Heating rate (°C/min)	Sintering time (min)
3β5-C5	1700	20	60
4β5-C5	1750	20	60
7β5-C5	1700	20	30
9β5-C5	1750	5	60
2β10-C5	1700	20	60
2β15-C5	1700	20	60
2β20-C5	1700	20	60

RESULTS AND DISCUSSION

The sample homogeneity was checked by SEM using back-scattered electrons. Fig. 10B show the microstructure of the 4β5-C5 sample, as an example. It is observed that the amorphous phase (bright areas) is uniformly distributed in the intergranular (β-SiAlON grains) region, showing that the milling process was suitable to provide a good component distribution.

Some samples show high porosity in the edge (Fig. 10A), due to Si_3N_4 decomposition, leading to samples with low density values (~ 92% theoretical).

The EDX grains analysis (Fig. 1 - dark phase of Fig. 10B) shows that actually the SiAlON compound was formed, e.g., Al was in solid solution with silicon nitride. The spectrum was obtained from samples with 5 and 15 eq% Al (β5-C5 and β15-C5 samples, respectively). It can be seen that the β15-C5 sample has much more Al inside the grains, in agreement with the semi-quantitative chemical analysis shown in Table 3.

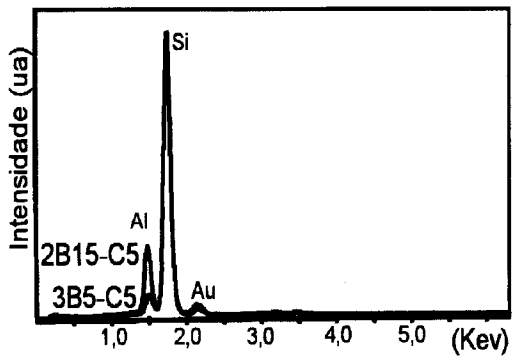

Figure 1 - EDX spectra measured inside the grains.

Table 3 - Results of semi-quantitative analysis, by EDX.

Sample	% equivalent	
	Al	Si
3β5-C5	4.7	95.3
2β15-C5	12.3	87.7

Composition influence: In order to study the effect of dopant concentration, tests were performed at 1700 °C for 60 minutes, with 20°C/min heating rate, for samples containing 5, 10, 15 and 20 eq% of Al and 5 wt.% of $(REC)_2O_3$.

During the heating process, all samples showed the same behavior (Fig. 2). At 1700 °C, samples containing 15 and 20 eq% of Al reached the largest length variation ($\Delta L/L_0$). By comparison with density values shown in Table 4, it is possible to conclude that increasing Al_2O_3 content, high densifications can be reached.

Fig. 3 shows the X-ray diffraction pattern of a sample with 5% eq Al. It is observed that this sample shows α-phase that disappears as the Al concentration increases.

SEM micrographs with secondary electrons in as-polished and chemically etched surfaces are depicted in Figs. 10C to 10F. Samples with 5 eq% Al and 5 wt% rare earth concentrate (Fig. 10C) show β-SiAlON grains with small aspect ratio. As the Al amount increases, β-SiAlON grains become smaller, more spherical and with more homogeneous size distribution. The Si-Al and N-O substitutions lead to a modification in the nucleation process and β-SiAlON phase growth, causing modification in the grain aspect ratio.

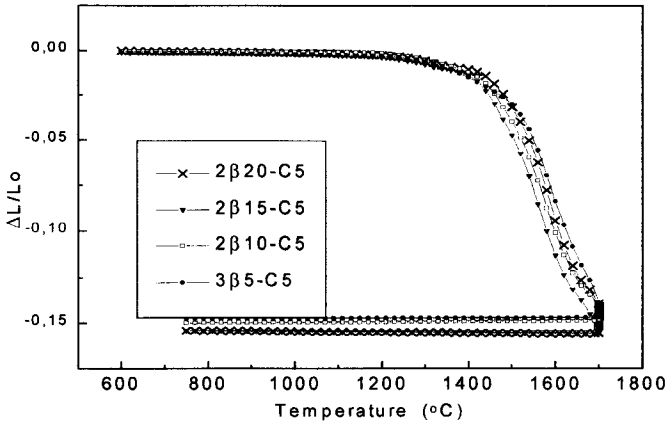

Figure 2 - $\Delta L/L_0$ plots. Samples with different compositions sintered at 1700 °C/60 min.

Table 4 - Density values variation versus concentration for sample sintered at 1700 °C/60 min.

Sample	% mass loss	% theoretical density
3β5-C5	2.48	93.27
2β10-C5	2.41	97.55
2β15-C5	2.5	98.46
2β20-C5	-	98.91

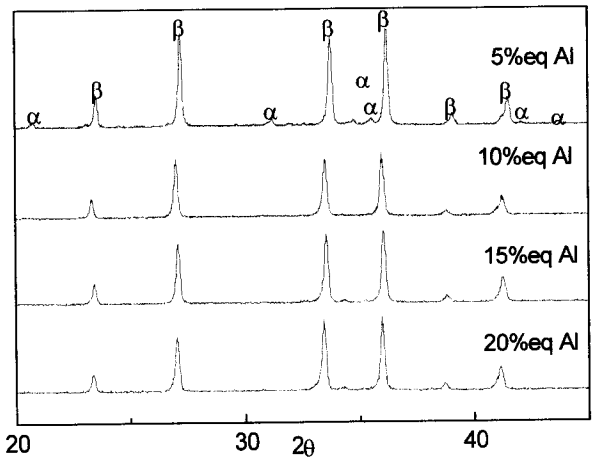

Figure 3 - X-ray diffraction patterns. Samples with different concentrations of Al sintered at 1700°C/60 min.

Variation of Heating Rate: the densification curves for different heating rates (5 or 20 °C/min) are shown in Fig. 4. The sample heated at 5 °C/min has an inflection in the 1200 - 1440 °C range, due to oxide liquid phase formation (Al_2O_3, SiO_2 and $(REC)_2O_3$), with higher densification at lower temperature. This sample shows the highest density value and the smallest mass loss (Table 5). After sintering, both samples showed full α - β transformation (Fig. 5).

The formation of large β-SIAlON grains and smooth surfaces result in an increase of the heating rate (Figs. 10G and 10H). This is probably due to the fact that the necessary condition for β-SiAlON nucleation and growth occurs later in some sites than in others. This happens because the temperature distribution is non-homogeneous for high heating rates.

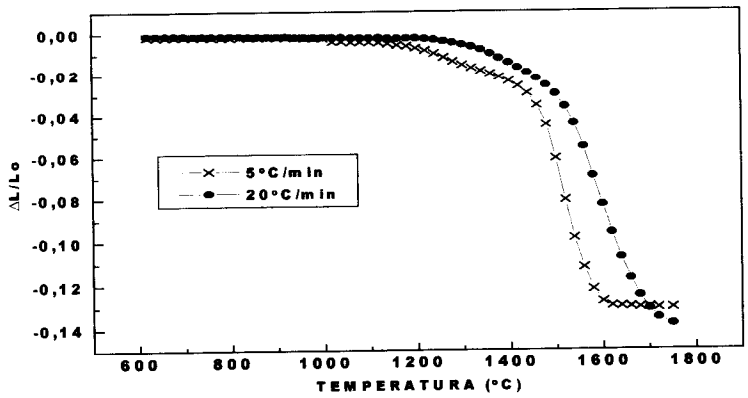

Figure 4 - $\Delta L/L_0$ plots. Samples containing 5 eq. % Al sintered at 1750 °C with different heating rates.

Table 5 - Heating rate, mass loss and % of theoretical density.

Sample	Heating rate (°C/min)	% mass loss	% theoretical density
9β5-C5	5	2.99	94.19
4β5-C5	20	3.34	92.35

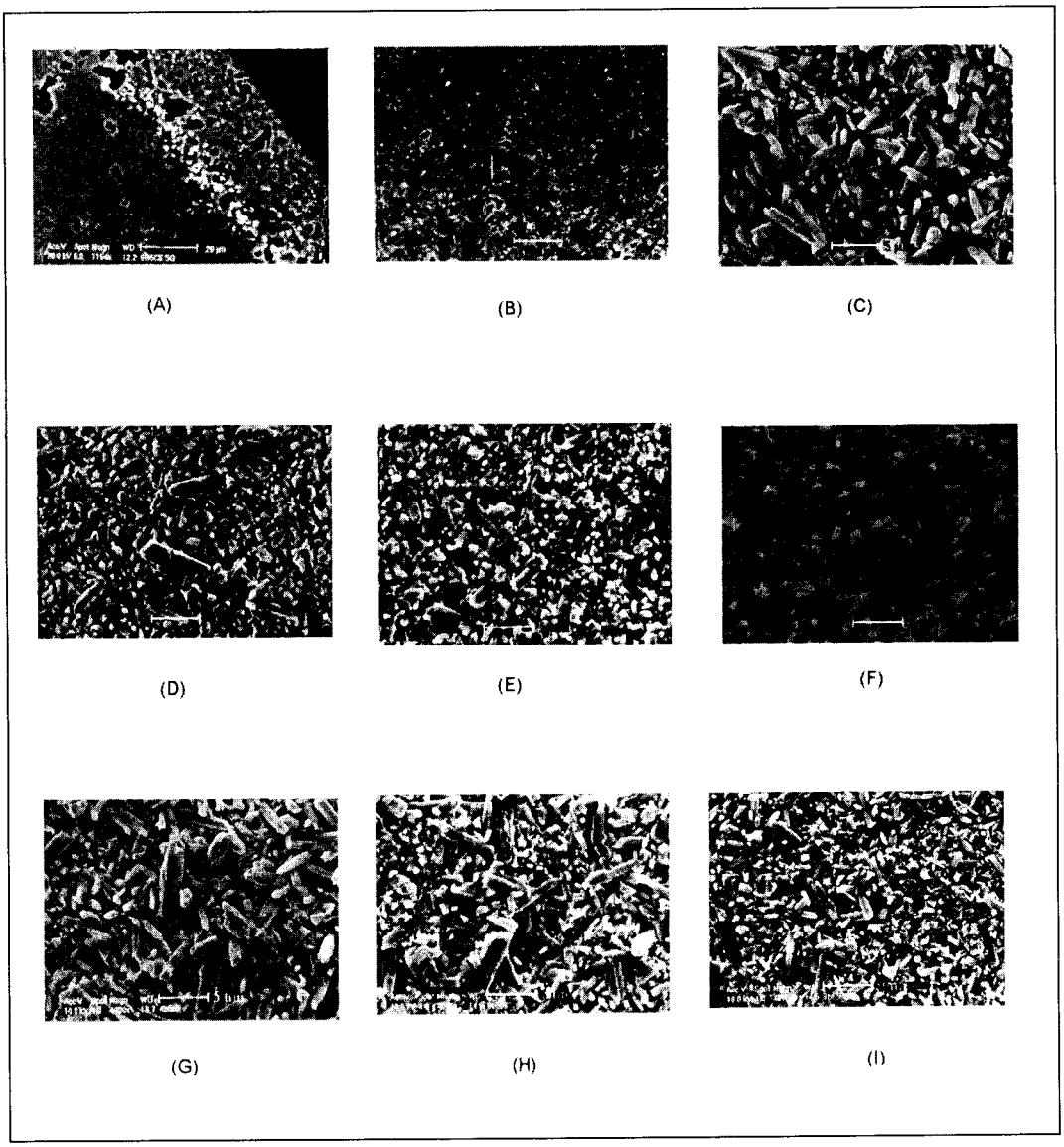

Figure 10 - SEM images of samples: (A) edge of sample 4β5-C5, (B) 4β5-C5 by back-scattered electrons and (C) 3β5-C5, (D) 2β10-C5, (E) 2β15-C5, (F) 2β20-C5, (G) 4β5-C5, (H) 9β5-C5, (I) 7β5-C5 by secondary electrons.

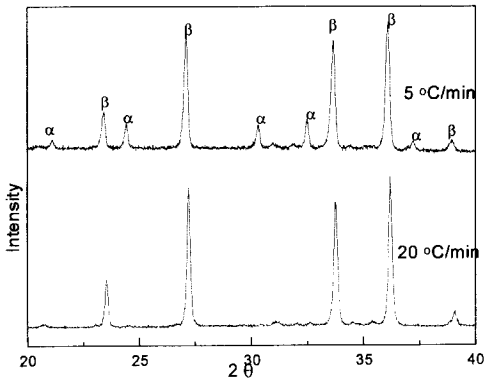

Figure 5 - X - ray diffraction pattern of sample containing 5 eq% Al, sintered at 1750 °C with different heating rates.

Different sintering temperatures: Fig. 6 shows densification curves for samples sintered at 1700 and 1750 °C/60 min, with 20 °C/min heating rate. Retraction curves are similar, with small retraction values up to 1700 °C. Table 6 shows that the sample sintered at 1750 °C has the lowest density value and the highest mass loss, due to Si_3N_4 decomposition. However, this sample had more α-β transformation (Fig. 7).

The increase in the final temperature leads to larger grain sizes (mainly grain diameter),as can be seen in Figs. 10C and 10G. This phenomenon is related to grain coalescence process. A proportional diameter increase is related to grain crosslinking, preventing in many cases, the longitudinal growth.

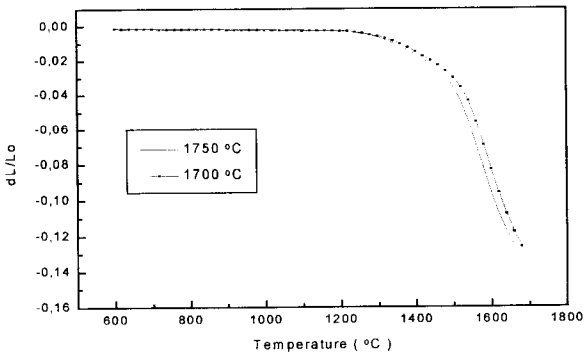

Figure 6 - $\Delta L/L_0$ plots. Sample containing 5 eq% Al sintered at different temperatures.

Table 6 - Density variation of the samples versus sintering temperature.

Sample	Temperature (°C)	% mass loss	% theoretical density
3β5-C5	1700	2.48	93.27
4β5-C5	1750	3.34	92.35

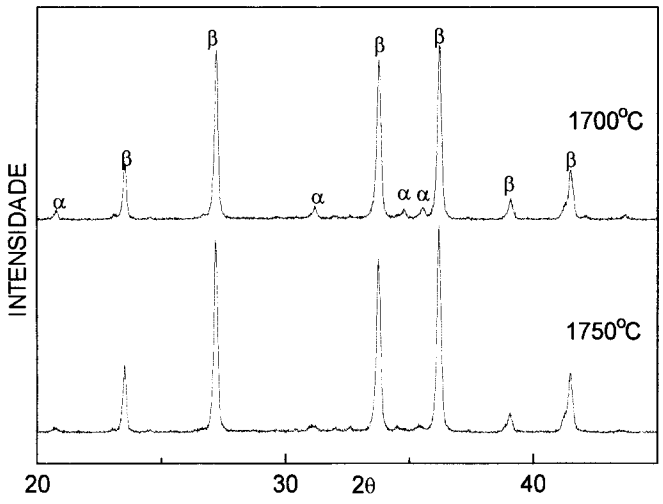

Figure 7 - X - ray diffraction pattern of sample with 5 eq% Al sintered at different temperatures.

Influence of Sintering Time: The influence of sintering time (30 and 60 min) was studied for samples sintered at 1700 °C. The curves (Fig. 8) show that the retraction behaviors are similar. However, the sample sintered at 1700 °C/30 min had higher density (Table 7). When sintering time is raised the quantity of β-phase increases (Fig. 9).

The micrographs (Figs. 10C and 10I) show that as the sintering time increases, so does the grain size due to the smaller grain dissolution and larger grain coalescence.

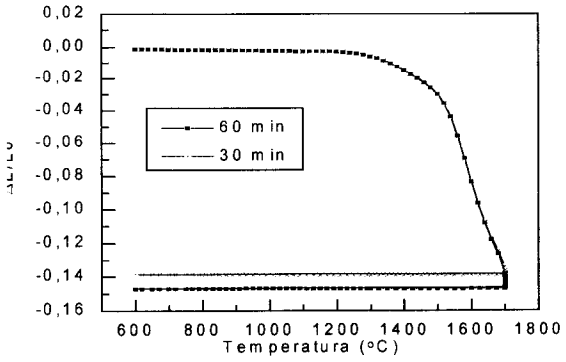

Figure 8 - $\Delta L/L_0$ plots. Sample sintered at 1700 °C for different times.

Table 7 - Density variation versus time sintering at 1700 °C.

Sample	Time of sintering (min)	% mass loss	% theoretical Density
7β5-C5	30	2.31	95.11
3β5-C5	60	2.48	93.27

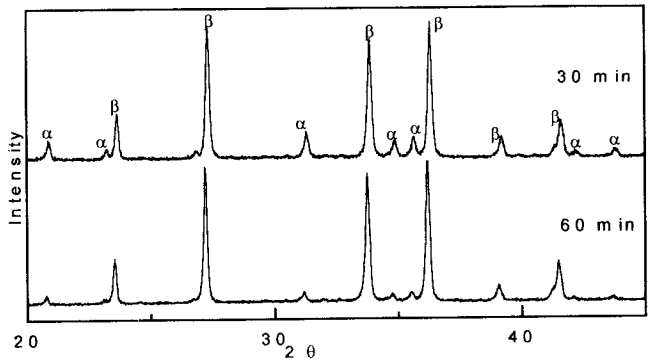

Figure 9 - X - ray diffraction pattern of sample with 5 eq% Al sintered at 1700 °C for different times.

CONCLUSIONS

The present work shows that the adopted mixing and milling processes lead to a high sample homogeneity and to an uniform distribution of liquid phases during sintering.

The addition of only rare earth concentrate to produce SiAlON by pressureless methods, leads to full density specimens with densities higher than 98 % of theoretical ones.

The densification and β-phase formation increase with increasing Al concentration. The Al and O play a role in β-SiAlON nucleation and growth mechanism, leading to smaller grain sizes and increased aspect ratio.

The final density depends on the heating rate, but the amount of transformed phase after sintering does not. It seems that it influences β-SiAlON nucleation and growth conditions, causing modifications in grain size and shape.

At 1700 °C there were low mass loss and higher final density comparing to 1750 °C. Better density results were obtained at 1700 °C for 30 min, although the α-β transformation has not been completed. The increase in sintering time and temperature lead to an increase in grain size due to the coalescence process, as expected.

ACKNOWLEDGEMENTS

The authors would like to tank to CNEN, PADCT/FINEP and CNPq for financial support and to Dr. J. R. Martinelli, J. Marchi and C. V. Moraes.

REFERENCES

[1] P.Vicenzini, 16 [1], 3-29 (1986).
[2] M. Knutson-Wedel, L. K. L. Falk, T. Ekström, T. V. 89-91. p 153-57. Trans Tech Publications Ltd, Switzerland (1994).
[3] J. Duailibi F., J. C. Bressiani, Mat. Sci. Eng. A 209 (1996) p. 164-68.
[4] Kuzjukevics, K. Ishizaki, J. Am. Ceram. Soc. 76 (1993) p. 2373-75.
[5] Y. Oyama Jap. J. Appl. Phys., 11 (1972) p. 750-51.
[6] R. A. L. Drew Can. Metall. Q., 27 (1988) p. 59-64.
[7] N. Sugiyama, Y Ukyo, S. Wada, J. Ceram. Soc. Japan, 101 (1993) p. 729-32.
[8] N-K Kim, D-Y Kim, A. Kranzmann, E. Bischoff, S-J. L. Kang, J. Mat. Sci.. 28 (1993) p. 4355-58.

Advanced Powder Technology I
doi:10.4028/www.scientific.net/MSF.299-300

Use of Rare Earth Concentrate as a SiAlON Sintering Additive
doi:10.4028/www.scientific.net/MSF.299-300.141